How the Co-C bond is cleaved in coenzyme B-12 enzymes: A theoretical study

Jensen, Kasper; Ryde, Ulf

Published in:
Journal of the American Chemical Society

DOI:
10.1021/ja050744i

2005

Document Version:
Peer reviewed version (aka post-print)

How the Co–C bond is cleaved in coenzyme B_{12} enzymes: a theoretical study

Kasper P. Jensen and Ulf Ryde

Department of Theoretical Chemistry
Lund University
Chemical Center
P. O. Box 12
S-221 00 Lund
Sweden

Correspondence to Ulf Ryde
E-mail: Ulf.Ryde@teokem.lu.se.
Tel: +46-46-2224502
Fax: +46-46-2224543

2017-04-09

Abstract

The homolytic cleavage of the organometallic Co–C bond in vitamin B_{12}-dependent enzymes is accelerated by a factor of ~10^{12} in the protein compared to the isolated cofactor in aqueous solution. To understand this much debated effect, we have studied the Co–C bond cleavage in the enzyme glutamate mutase with combined quantum and molecular mechanics methods. We show that the calculated bond dissociation energy (BDE) of the Co–C bond in adenosyl cobalamin is reduced by 135 kJ/mol in the enzyme. This catalytic effect can be divided into four terms. First, the adenosine radical is kept within 4.2 Å of the Co ion in the enzyme, which decreases the BDE by 20 kJ/mol. Second, the surrounding enzyme stabilizes the dissociated state by 42 kJ/mol using electrostatic and van der Waals interactions. Third, the protein itself is stabilized by 11 kJ/mol in the dissociated state. Finally, the coenzyme is geometrically distorted by the protein and this distortion is 61 kJ/mol larger in the Co^{III} state. This deformation of the coenzyme is caused mainly by steric interactions and it is especially the ribose moiety and the Co–C5'–C4' angle that are distorted. Without the polar ribose group, the catalytic effect is much smaller, e.g. 42 kJ/mol lower for methyl cobalamin. The deformation of the coenzyme is caused mainly by the substrate, a side chain of the coenzyme itself, and a few residues around the adenosine part of the coenzyme.

Key words: coenzyme B_{12}, cobalamin, Co–C bond dissociation, glutamate mutase, QM/MM, density functional theory.

Introduction

Cobalamins (vitamin B_{12} derivatives) are among the most complex cofactors in biology in terms of molecular weight and the number of functional groups. As can be seen in Figure 1, it consists of a tetracyclic ring system, corrin, which resembles heme except that one of the methine bridges between the rings is missing and ten of the outer carbon atoms are saturated. In the center of this ring, a cobalt ion is bound. The two functional forms, adenosyl and methyl cobalamin (AdoCbl and MeCbl), contain a 5'-deoxyadenosyl (Ado) group or a methyl (Me) group, respectively, bound to the Co ion by a Co–C bond. This makes cobalamins the only well-documented organometallic cofactors in nature.[1] In these forms, cobalt is in the Co^{III} oxidation state, but during catalysis it attains the Co^{II} or Co^{I} oxidation states, with cobalt always being in the low-spin state.[2] On the periphery of the corrin ring, several side chain are bound, mostly methyl, acetamide, and propionamide groups. However, one of the side chains is much longer and ends with a 5,6-dimethylbenzimidazole group, which coordinates to the cobalt ion as an axial ligand in the free cobalamins and also in some enzymes (e.g. the dehydratases)[3]. In other enzymes, e.g. the two human B_{12} enzymes, methionine synthase[4] and methylmalonyl coenzyme A mutase[5] (MCAM), it is replaced by a histidine (His) ligand from the protein.[6]

AdoCbl is the cofactor of several enzymes, such as MCAM, glutamate mutase (GluMut)[7], methyleneglutarate mutase,[8] class II ribonucleoside triphosphate reductase, ethanolamine ammonia lyase,[9] and diol- and glycerol dehydratase.[10] A common feature of these enzymes is that the Co–C bond of AdoCbl is cleaved homolytically to initiate the reaction, giving rise to a five-coordinate Cob(II)alamin and an Ado radical. The Ado radical subsequently initiates radical-based rearrangements of the substrate, typically 1,2-shifts at saturated hydrocarbon centers. Thus, these reactions are initiated by cleavage of the organometallic Co–C bond.[11]

Kinetic studies have shown that homolysis of isolated AdoCbl in aqueous solution is very slow, with rates of 10^{-9} s^{-1} at 25° C, corresponding to a half-life of 22 years.[12] The Co–C bond dissociation energy (BDE) has been estimated to be 126 ± 8 kJ/mol.[12,13] Likewise, the equilibrium constant for AdoCbl homolysis is very small, $7.9 \cdot 10^{-18}$ M.[14,15] On the other hand, several coenzyme B_{12} enzymes attain catalytic rates (k_{cat}) of 2–300 s^{-1} ($\Delta G^{\ddagger} \approx 60$ kJ/mol).[12,15,16,17,18,19] Thus, these enzymes seem to increase the rate of Co–C bond homolysis by 12±1 orders of magnitude[12,19] and lower $\Delta G^{\ddagger}$ by ~60 kJ/mol.[14,15,19] Although there is a general agreement of this change in $\Delta G^{\ddagger}$, no consensus has been reached whether the decrease is mainly enthalpic, entropic, or both.[17,18,19] Furthermore, the enzymes shift the equilibrium constant towards the homolysis products by a factor of $3 \cdot 10^{12}$ (74 kJ/mol), giving an equilibrium constant close to unity in the enzyme.[14,16,20,21,22] However, for all the studied enzymes, homolysis of the Co–C bond is not the rate-limiting step and this homolysis is kinetically coupled to the transfer of the radical from Ado to the substrate or to a protein residue.[16,20,21,23,24]

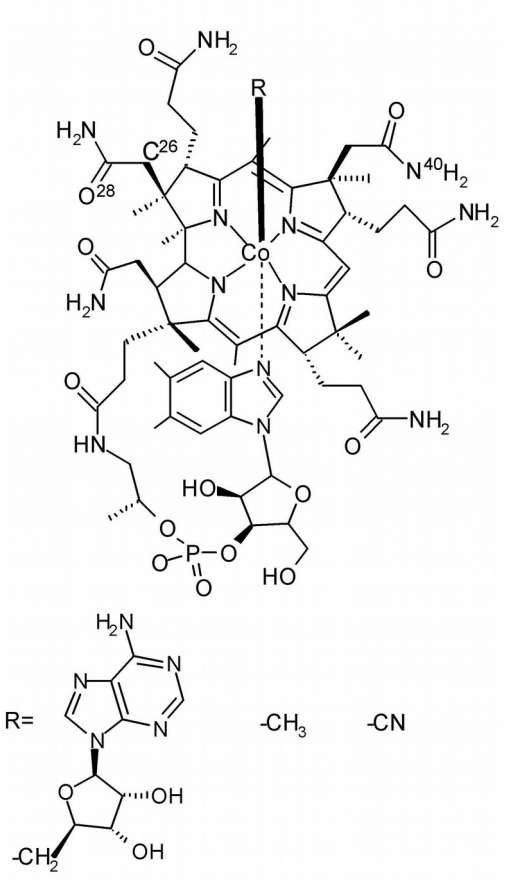

Figure 1. The cobalamin system.

The cause of these large catalytic enhancements has been much discussed, in particular the unique labilization of the organometallic Co–C bond, and it is one of the most important unsolved problems in bioinorganic chemistry. Many different mechanistic explanations have been suggested. It has been proposed that the enzyme may compress the axial Co–N_{Im} bond, causing upwards folding of the corrin ring and strain in the Co–C

bond[25,26,27], the so-called mechanochemical trigger mechanism. However, recent theoretical calculations from several groups have shown that reasonable compressions cannot destabilize the Co–C bond significantly[28,29,30]. Raman spectroscopy also speaks against any effect of the corrin ring in Co–C bond labilization.[31] In addition, crystal structures of various enzymes do not show any compression of the Co–N_{Im} bond.[32] On the contrary, most crystal structures of B_{12} enzymes show Co–N_{Im} bonds that are longer than for the isolated cobalamins and a flattening of the corrin ring.[4,5,28,33] It has subsequently been suggested that a *lengthening* of the Co–N_{Im} bond could selectively stabilize the Co^{II} oxidation state[5,34]. Yet, many experimental and theoretical data speak against such a suggestion as well.[28,35,36,37] Moreover, mutation of the His ligand in GluMut leads only to a 1000-fold decrease in $k_{cat.}$[38] This shows that the axial *N*-base can at most enhance the reaction by 15 out of ~60 kJ/mol.

Other suggestions also rely on steric and electronic strain of the resting state of AdoCbl, owing to interactions involving the corrin ring and its side chains,[11,14] twisting the axial Co–N_{Im} bond,[39] or that the protein may pull or tilt the Co–C bond by directly interacting with the Ado group.[31,39,40,41,42,43,44] Primary isotope effects indicate a coupling of the Co–C bond cleavage and hydrogen transfer, which may provide additional driving force for Co–C bond cleavage.[16,20,21,23,24] Finally, it has been suggested that the catalysis comes from the preferential binding of the homolysis products and that the binding site of AdoCbl is disrupted by the binding of the substrate.[12,40,45]

Recently, several groups have started to use density functional calculations to acquire insight into the reactivity of cobalamins. Whereas studies of the radical reactions subsequent to Co–C bond cleavage have been pursued both in vacuum[46,47,48,49,50] and in two proteins,[51,52] inclusion of the entire corrin ring to study questions regarding the actual role of the cofactor is more recent.[28,29,53,54,55,56,57] It has been shown that the Co–C bond dissociation energy is linearly related to the Co–C bond length and that it is little affected by variations in the Co–N_{Im} bond length or the type of axial ligand, including a deprotonated histidine.[28,55] A recent combined quantum and molecular mechanics (QM/MM) study showed that this is the case also in MCAM.[58]

In this paper, we study the Co–C bond cleavage in GluMut. GluMut (EC 5.4.99.1) catalyzes the stereospecific conversion of *S*-glutamate to (2*S*,3*S*)-3-methylaspartate (MeAsp), shown in Figure 2.[59] We investigate how GluMut enhances the cleavage of the Co–C bond using QM/MM methods. We show that the protein in the closed, substrate-bound, form strongly destabilizes the Co–C bond. Moreover, we investigate which energy components, which residues in the protein, and which groups in the coenzyme are involved in this destabilization. Together, these results give a quite clear picture of this much-debated enzymatic reaction.

Methods

QM/MM procedure

The QM/MM simulations were carried out with the ComQum software.[60,61] In this approach, the protein is divided into three regions: System 1 is optimized by quantum chemistry, system 2 is optimized by molecular mechanics (MM) methods, whereas system 3 is kept fixed at the crystal coordinates. Covalent bonds between systems 1 and 2 are treated by the link-atom approach,[62] indicating that the quantum system is truncated by hydrogen atoms, the positions of which are directly related to those of the corresponding heavy atoms in the

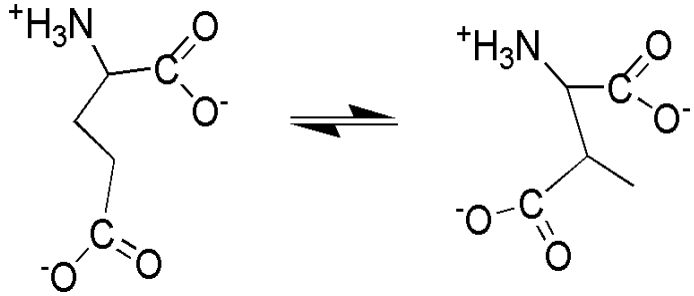

Figure 2. Conversion of glutamate to MeAsp, catalyzed by glutamate mutase.

protein.[60]

The total QM/MM energy is calculated as:

$$E_{QM/MM} = E_{QM1} + w_{MM}(E_{MM123} - E_{MM1}) \quad (1)$$

Here, E_{QM1} is the quantum mechanical (QM) energy of system 1 with H link atoms, including all the electrostatic interactions between the quantum system and the surroundings (the protein is included in a self-consistent manner, modeled as an array of point charges, one for each atom, taken from the Amber force field,[63] but charges of atoms directly bound to the link atoms are removed). Similarly, E_{MM1} is the MM energy of system 1, still with H link atoms, but without any electrostatic interactions. Finally, E_{MM123} is the classical energy of systems 1–3 with no link atoms and electrostatic interactions only outside the quantum system 1. Thereby, the total energy should represent a system without any link atoms and effects of the link atom truncation should cancel out. This approach is similar to the one used in the ONIOM method.[64] The w_{MM} factor provides a weight between the QM and MM forces and energies. It is 1 in normal QM/MM calculations, but can be reduced if one wants to estimate the effect of the protein.

The geometry optimizations were carried out in two steps. First, systems 2 and 3 were frozen and only the quantum system was optimized. Second, both systems 1 and 2 were allowed to relax. During this optimization, the charges on the quantum atoms in the MM minimization were obtained from the QM calculations and were updated in each iteration of the optimization. These calculations were performed with the looser convergence criterion of 10^{-4} a.u. (0.26 kJ/mol) for the change in energy and 10^{-2} a.u. (0.50 kJ/mol/pm) for the maximum norm of Cartesian gradient. Then, system 2 was frozen again and the geometry optimization was continued with default convergence criteria (10^{-6} and 10^{-3} a.u.). Such an approach was followed to get a feeling of the relaxation of the surrounding protein, but also to minimize artifacts caused by shortcomings of the MM force field. If not otherwise stated, the discussion is based on the results obtained with the protein free to relax, because these structures are expected to be more realistic.

The protein

All calculations in this paper are based on the recent crystal structure of GluMut crystallized with the glutamate substrate (although the structure contains mainly the product, MeAsp), protein data bank entry 1i9c (1.9 Å resolution).[65] This structure was chosen because it contains the native AdoCbl coenzyme (in variance to the other two available crystal structures of GluMut[66]) and it shows the enzyme in the active closed (substrate-bound) form. GluMut is a dimer, in which each subunit consists of two peptide chains, one that binds the substrate and one that provides the His ligand of AdoCbl.[67] In the calculations, we used only the A and B chains of one subunit, plus all residues and crystal water molecules of the other subunit within 27 Å from the C5' atom in the Ado residue (viz. residues 300–313 and 341–357; the Co–Co distance between the two subunits is 43 Å), cf. Figure S1. In total, 654 residues were treated in the calculations, including one molecule of AdoCbl and one glutamate substrate molecule. The protein was solvated in a sphere of water molecules with a radius of 30 Å, centered on the C5' atom (in total 1017 water molecules), giving a total of 13352 atoms in the calculations.

Hydrogen atoms were added to the protein, assuming the normal protonation status at pH 7.0 for the Asp, Glu, Lys, and Arg residues. After a detailed study of the surroundings and possible hydrogen-bond networks around the His residues, it was decided that His-16 and 300 are protonated on the $N^{\delta 1}$ atom, whereas His-212, 287, and 428 are protonated on the $N^{\varepsilon 2}$ atom, and the remaining five His residues are doubly protonated (and therefore positively charged). The hydrogen atoms and the solvation water molecules were optimized by a simulated annealing calculation by molecular dynamics, using the Amber 7 software and the Cornell force field.[84,68] For cobalamin, we employed the parameters of Marques and Brown.[69]

The quantum system included the corrin ring (without any side chains, Cor), the imidazole (Im) side chain of the His-16 ligand, and the whole Ado group (84 atoms), cf. Figure S2. For calculations on the radical-transfer step, we included also the glutamate substrate in the quantum system, giving 102 atoms. In system 2, all residues within 10 Å of any atom in the quantum system were included (always whole amino acids; 2353 atoms; Figure S3). System 3 consisted of the rest of the included parts of the enzyme (10915 atoms).

Test calculations with a smaller and a larger system 2 (6 Å = 1117 atoms or 15 Å = 5023 atoms) were also performed. Some small changes in the geometry were observed when going from 6 to 10 Å, whereas the relative QM/MM energies hardly changed. With the largest system 2, no significant change in the geometry was observed. Therefore, most of the presented results were obtained with the 10-Å system 2. We also tested to run a short molecular dynamics simulation of system 2 (12 ps at 300 K) before the minimization in each of the first 40 steps of the geometry optimization (to allow a larger relaxation of system 2). However, this did not have any significant effect on the geometries or energies.

To evaluate the effect of various parts of the protein on the binding equilibrium between Co^{III} and Co^{II}, we also optimized structures of a number of mutants, in which one or several residues were replaced by glycine.

Quantum chemical calculations

The QM calculations were carried out with the Turbomole software,[70] version 5.6.[71] We employed the 6-31G(d) basis set for all atoms except cobalt, which was described by the DZP basis set of Schäfer *et al*.[72] This basis set assigns one set of polarization functions to all non-hydrogen atoms. Only the pure five *d*-type functions were used. We applied the default (m3) grid size of Turbomole and the calculations were sped up by expansion of the Coulomb interactions in auxiliary basis sets, the resolution-of-identity approximation.[73,74] Unrestricted calculations were performed for all calculations, except at the equilibrium Co^{III} state.

The strength of the Co–C bond was measured as the (homolytic) bond dissociation energy (BDE). We calculate the BDE as the energy of the reaction

$$Co^{III}CorImAdo^{+} \rightarrow Co^{II}CorIm^{+\bullet} + Ado^{\bullet} \qquad (2)$$

Previous theoretical calculations have shown that the standard B3LYP functional gives too low calculated values for this BDE.[75] Therefore, we used the density functional Becke–Perdew86 method[76,77] for both geometry optimization and evaluation of energies at various Co–C bond distances. We have shown that this procedure provides geometries and Co–C bond strengths in good agreement with experiment.[75] In the QM/MM calculations, the BDE was estimated by gradually increasing the Co–C bond length and relaxing the surrounding protein (systems 1 and 2).

In order to estimate the effect of the electrostatic field of the surrounding enzyme on the quantum system, we calculated the energy of the quantum system in vacuum but at the geometry obtained in the protein (by QM/MM). The difference between this energy and that of the quantum system optimized in vacuum is denoted ΔE_{QM1} and describes how much the quantum system is geometrically distorted in the enzyme. This energy is often called strain energy, but it contains many interactions that are normally not considered as strain, in particular electrostatic effects.[78]

Results and Discussion

Optimized structures

In order to judge the performance of our QM method, we have optimized the geometry of the AdoCbl cofactor in vacuum. The results in Table 1 show that the theoretical structure agrees with experiments to within 0.04 Å.[79] However, the calculated fold angle is 8° smaller than in the crystal structure. This probably reflects the fact that the fold angle is a low-energy mode that is determined mainly by the packing of the corrin side-chains in the crystal. Similar results are also obtained for the reduced coenzyme (Co^{II}CorIm).[80]

The crystal structure of GluMut we have employed in our calculations originally contained AdoCbl and the glutamate substrate.[66] However, the electron-density map was interpreted as a mixture of glutamate (30%) and the product MeAsp (70%). Likewise, two conformations of the Ado group are seen, both practically dissociated from the Co ion. In conformation B (40% occupancy), the C5' atom is directed towards the Co ion at a Co–C distance of 3.17 Å. In the other conformation (60% occupancy), C5' is displaced towards the substrate, forming a van der Waals contact with it. Consequently, the Co–C distance has increased to 4.19 Å. This is accomplished by a change in the puckering of the ribose ring from C3'-endo to C2'-endo and a small rotation around the glycosidic bond. In our calculations, we

deleted the MeAsp molecule and run separate calculations starting from both conformation A and B of the Ado group.

The optimized QM/MM structures of AdoCbl in GluMut are also included in Table 1. The calculation started with conformation B (min2) ended up with a Co–C distance of 3.48 Å, i.e. somewhat longer than in the crystal structure, which is not unexpected for such a non-bonded distance with disorder in the crystal structure. On the other hand, the Co–N distances (for which the crystal structure gives only one conformation) are well reproduced in the calculations, except for the strange longest $Co–N_{Cor}$ bond in the crystal structure (2.02 Å), which is 0.05 Å shorter (and therefore more reasonable) in the calculations. Even the corrin fold angle is well modeled: We obtain an almost flat corrin ring with a fold angle of 3 °, whereas the experimental fold angle is 2° for both conformations. Flattening of the corrin fold angle upon entering the protein is consistent with Raman spectroscopic studies.[81] This supports our suggestion that the large fold angle for the isolated cofactor is caused by crystal-packing effects. It also shows that the fold angle is a low-energy mode and hence speaks against any trans steric effect in cobalamin-dependent enzymes, as has been pointed out earlier.[28]

The structure started in conformation A (min3) gave a longer Co–C distance of 4.01 Å, in reasonable agreement with the crystal structure (4.19 Å) considering that there is no bonding interaction at this distance. The Co–N bond lengths are virtually identical to those of the other conformation, as is also suggested by the crystal structure. The ribose ring has also retained the changed puckering in the crystal structure.

In both crystal conformations, N1 and N3 of the adenine moiety form hydrogen bonds to one water molecule each, whereas the two hydrogen atoms on N6 form hydrogen bonds to the back-bone carbonyl oxygen atom of Gly-68 and Asn-123, and N3 is hydrogen bonded to one of the side chains of coenzyme B_{12} (N40), as can be seen in Figure 3a. Conformation B is stabilized by a hydrogen bond between O2' and a side-chain amide oxygen of the corrin ring (O28), and by hydrogen bonds between O3' and a water molecule, Lys-326, and Glu-330. In our QM/MM structure based on the former conformation (min2), this hydrogen-bond structure is quite well retained. The most notable difference is that the hydrogen bond between O3' and Glu-330 has become very strong (1.43 Å), with a concurrent weakening of the hydrogen bond to the water molecule. In conformation A, the ribose moiety has altered its conformation so that it instead forms two strong hydrogen bonds between the O2' and O3' atoms and the two carboxylate oxygen atoms of Glu-330 (Figure 3b). These interactions are retained in the QM/MM structure.

Table 1. Optimized structures of cobalamin models and the active site in GluMut compared to experimental data.[a]

System	Method	Co–C	$Co–N_{Im}$	$Co–N_{Cor}$				Fold angle	Co–C–C
Co^{III}CorImAdo	vacuum[b]	2.01	2.20	1.88	1.88	1.94	1.94	5.1	119.2
AdoCbl	exp.[79]	2.03	2.24	1.88	1.88	1.92	1.92	13.3	123.4
Co^{II}CorIm	vacuum[b]	–	2.14	1.87	1.88	1.93	1.94	6.0	–
Cob(II)alamin	exp.[80]	–	2.13	1.89 (average)				16.3	–
GluMut, min1[c]	QM/MM	2.09	2.49	1.87	1.92	1.94	1.94	4.8	138.0
GluMut, min2[d]	QM/MM	3.48	2.19	1.87	1.90	1.93	1.97	3.0	131.6
GluMut, min3[e]	QM/MM	4.01	2.18	1.87	1.89	1.92	1.97	3.6	102.8
GluMut	exp.[66]	3.17 4.19	2.22	1.88	1.90	1.93	2.02	1.6	162.0 104.3

[a] Bond lengths in Å; angles in degrees.
[b] Cobalamin models optimized in vacuum (i.e. without any surrounding protein).
[c] A Co^{III} minimum with a short Co–C bond length.
[d] A Co^{II} minimum with a long Co–C bond, but with the ribose in the C3'-endo state, corresponding to the B conformation in the crystal structure.
[e] A Co^{II} minimum with a long Co–C bond and with the ribose in the C2'-endo state, corresponding to the A conformation in the crystal structure.

We have also found a Co^{III} structure for AdoCbl in GluMut, which is interesting, because there is no crystal structure available for this state in GluMut. The energy of this structure is slightly lower (13 kJ/mol) than the dissociated states, suggesting an equilibrium constant close to unity. The structure is shown in Figure 4a and it has a Co–C bond length of 2.08 Å, i.e. slightly longer than in the vacuum structure. In contrast to the Co^{II} states, the Co^{III} state has a long Co–N_{Im} bond of 2.50 Å. This is interesting, because such long bond lengths have been observed in many crystal structures, but usually for what has been interpreted as reduced states.[5,40,82] The fold angle is predicted to be 5°, i.e slightly larger than in the Co^{II} states. Thus, there is a small effect on corrin folding, but it is not energetically significant. A conspicuous feature of this structure is that the Co–C5'–C4' angle is appreciably larger (138°) than in the structures of the isolated cofactor (119° optimized and 123° in the crystal; Co–C–C in Table 1). Both experimental and theoretical results have suggested that the enzyme may activate the Co–C bond by changing this angle.[31,44] The hydrogen-bond interactions between the Ado group and the surrounding protein of the Co^{III} state are identical to those of conformation B of the Co^{II} state (Figure 4b).

Co–C Bond Cleavage

We have studied the cleavage of the Co–C bond by optimizing the $CoCorImAdo^{+}$ model with the Co–C bond constrained to various distances between 2.0 and 4.0 Å, starting from conformation B. These Co–C bond dissociation curves in vacuum and in the protein are shown in Figure 5. The vacuum curve is similar to what have been published before for MeCbl and AdoCbl,[29,83] (although the total BDE varies with the QM method used[75]). Interestingly, the vacuum curve gives only an energy difference of 125 kJ/mol between 2.0 and 4.0 Å, although the isolated products give a BDE of 143 kJ/mol. This effect has been observed before by Dölker et al., who explained it by the favorable interactions between the hydroxyl groups of the ribose moiety and the corrin ring.[83] This is supported by the fact that CoCorImMe (without any polar groups) attains 154 kJ/mol of the BDE of 160 kJ/mol at the same Co–C distance (4.0 Å). Dölker et al. argued that this effect is important also in the protein, where it is enhanced by interactions also with the surrounding enzyme.[83] In fact, they obtained a stabilization of 51 kJ/mol if the substrate and three residues of the protein were added to the model. This effect is treated in a more objective way in our QM/MM calculations, which include the whole protein and not only a few selected residues.[84,85]

The bond dissociation curve in the protein differs substantially from that obtained in vacuum (Figure 5). In particular, the Co^{III} state has been strongly destabilized by the enzyme, so much that the dissociated complex is only 13 kJ/mol less stable than the bound Co^{III} form. Thus, we find that the protein changes the Co–C BDE by 143 – 13 = 130 kJ/mol. Spin densities (Figure S4) confirm that the Co–C bond cleavage is homolytic and the reaction is virtually completed at Co–C = 3.5 Å.

The structural changes during the Co–C bond dissociation process are shown in Table 2. As can be seen from the comparison of the QM/MM structures of the Co^{III} state at Co–C = 2.0 Å and the Co^{II} state at 3.5 Å in Figure 6, the Co^{III} structure is quite distorted. In particular, the Co–N_{Im} bond is elongated (2.54 Å) and the C5'–Co–N_{Im} angle is far from straight (162°, compared to 173° in the optimized vacuum structure). This distortion is caused by movements

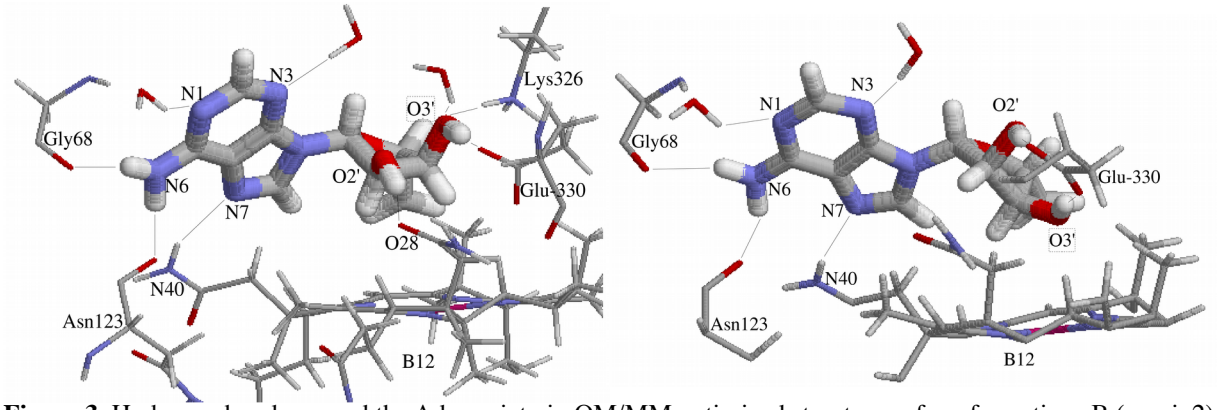

Figure 3. Hydrogen bonds around the Ado moiety in QM/MM optimized structures of conformations B (a; min2) and A (b; min3). The hydrogen bonds are marked out by thin lines.

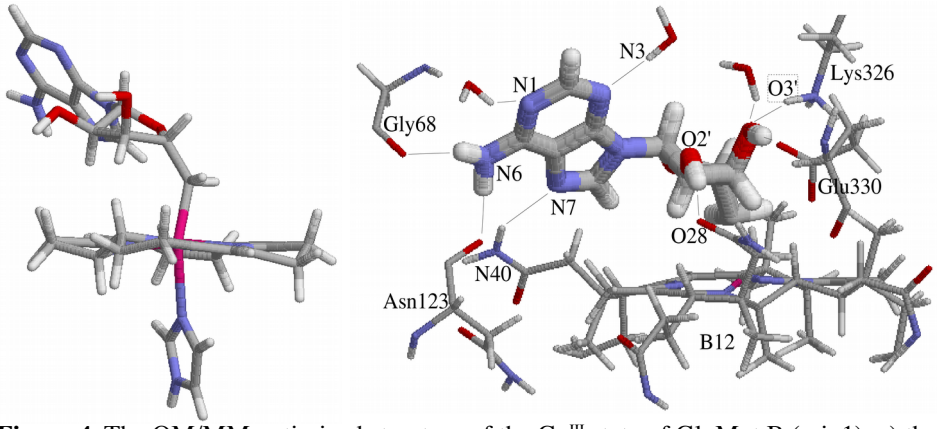

Figure 4. The QM/MM optimized structure of the Co^{III} state of GluMut B (min1): a) the quantum system; b) hydrogen bond interactions with the Ado group.

of the Co ion (0.47 Å) and the ribose moiety (average movement 0.64 Å; 1.14 Å for C5'). The corrin ring (0.15 Å), the adenine moiety (0.23 Å), and especially the His ligand (0.09 Å) do not change much between the two structures. When the Co–C bond is broken, Co moves closer to the corrin ring plane and the His ligand, leading to a normal length (2.19 Å) of the $Co–N_{Im}$ bond. This indicates that the position of the Ado moiety is restricted by the protein, leading to a large geometric effect in the most flexible part of the system, i.e. the $Co–N_{Im}$ bond.

Reasons for enhanced Co–C bond cleavage

In the following we will evaluate the effect of the protein as the difference between the structures obtained at Co–C distances of 2.0 and 3.5 Å (close to the vacuum minimum and the QM/MM min2),[86] for which the QM/MM energy difference is 8 kJ/mol in favor of the Co^{III} state. The total effect of the protein on the Co–C BDE is 143 – 8 = 135 kJ/mol. The aim of this and the following sections is to understand this major effect: What interactions are involved? What atoms in AdoCbl are affected? What residues in the protein cause this effect? We will start with the first question and note that we already have seen that a part of this effect (143 – 122 = 20 kJ/mol at 3.5 Å) can be attributed to the fact that the Ado radical does not dissociate from the enzyme, but instead interacts with the corrin ring with hydrogen bonds and other interactions that are improved when the Co–C bond is elongated, a sort of cage effect.[12]

We can directly use our calculations to divide the remaining effect (122 kJ/mol) into various energy components. First, we can use Eqn. (1) to divide the total QM/MM energy into the QM and MM parts (i.e. E_{QM1} and $E_{MM123} – E_{MM1}$, respectively). These curves are presented in Figure 7 (QM+ptch and MM), and they show that these two energies (relative to the dissociated state at 3.5 Å) have different signs: The QM+ptch term is negative (–33 kJ/mol at 2.0 Å) and is similar to the vacuum curve, although shifted towards less negative values. On the other hand, the MM term is positive (+25 kJ/mol at 2.0 Å) and thus counteracts the Co^{III} state. This term includes the van der Waals interaction between the quantum system and the surrounding protein and also the internal MM energy difference of the protein (system 2) between the two states at Co–C = 2.0 and 3.5 Å (including electrostatic effects outside system 1).

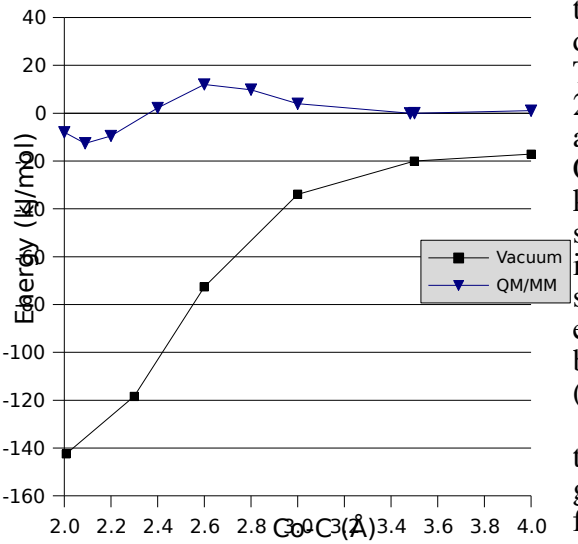

Figure 5. Co–C homolytic cleavage in glutamate mutase (QM/MM energy) compared with vacuum energies for $CoCorImAdo^+$. The reference energy is at 3.5 Å for the QM/MM curve, but at infinite separation in vacuum.

We can further divide the QM energy into two contributions, one coming from the geometry change of the QM system and one from the polarizing effect of the surrounding enzyme. This is done by recalculating the energies of each structure without the point-charge model of the enzyme. This curve is also included in Figure 5 (QM–ptch). It follows the QM+ptch line, but is more negative, especially

Table 2. Structural and energetic changes in the active site of GluMut when the Co–C bond is cleaved.[a]

Co–C[b]	Co–N_{Im}	Co–N_{Cor}	Fold angle	Co–C–C	ΔE^c
2.00	2.54	1.87 1.92 1.94 1.94	4.9	138.2	-7.9
2.08[d]	2.50	1.87 1.92 1.94 1.94	4.8	138.5	-12.7
2.20	2.46	1.87 1.92 1.92 1.94	4.7	137.4	-9.4
2.40	2.41	1.87 1.92 1.93 1.94	5.1	136.1	2.3
2.60	2.37	1.87 1.91 1.93 1.94	4.8	135.9	12.1
2.80	2.32	1.87 1.91 1.93 1.95	4.7	136.4	9.9
3.00	2.27	1.87 1.90 1.93 1.96	3.6	136.0	4.0
3.48[e]	2.19	1.87 1.90 1.93 1.97	3.0	131.6	0.0
4.00	2.16	1.87 1.89 1.93 1.98	2.9	124.5	1.1

[a] Bond lengths in Å; angles in degrees.
[b] The structures were obtained by QM/MM optimizations with the Co–C bond length fixed.
[c] The total QM/MM energy (kJ/mol), relative to the state with a Co–C bond length of 3.48 Å (min2).
[d] This is a fully optimized state, corresponding to min1 in Table 1 (i.e. the Co–C bond length was not fixed).
[e] This is a fully optimized state, corresponding to min2 in Table 1 (i.e. the Co–C bond length was not fixed).

at shorter Co–C bond lengths (–34 kJ/mol at 2.0 Å). This curve is directly comparable to the vacuum curve and shows the effect of the change in geometry of the cofactor in the protein. At 2.0 Å, the difference in energy between these two curves is 56 (122 – 66) kJ/mol, which is a direct measure of the geometric effect in the QM region of the coenzyme.

Likewise, the difference between the QM+ptch and QM1–ptch curves provides an estimate of the direct electrostatic (polarizing) effect of the surrounding enzyme on the cofactor. We can see that this effect is quite small. At Co–C = 2.0, it attains its maximum, 34 kJ/mol. It includes the differential stabilization of the Co^{II} state by electrostatic interactions with the surrounding protein. Thus, it provides a better estimate of the electrostatic effect of the protein than that obtained by Dölker et al.,[83] using only three residues of the protein. [87]

We can understand this 34-kJ/mol electrostatic stabilization in atomic detail by calculating the contributions of each atom and amino acid in the protein to the differential electrostatic stabilization of the 2.0 and 3.5 Å states (by modeling the two states with their QM charges). Such a calculation shows that the largest contributions come from Arg-66 (17 kJ/mol), Lys-326 (12 kJ/mol), Asp-14 (11 kJ/mol), the substrate (6 kJ/mol), and Gly-68 (5 kJ/mol; the total effect in this simplified model is 39 kJ/mol, i.e. 5 kJ/mol too large). A water molecule and Arg-100 provide the largest negative contributions (i.e. stabilizing the Co^{III} state by 4–5 kJ/mol). Asp-14 forms a hydrogen bond to the His ligand of Co, which is improved by 0.01 Å in the Co^{II} state. All the other groups interact with the ribose moiety, but also for these is the actual improvement quite small (e.g. 0.06 Å for the hydrogen between O3' of ribose and HN in Lys-326). Thus, these results show that the major electrostatic effects come from the interactions with the ribose moiety.

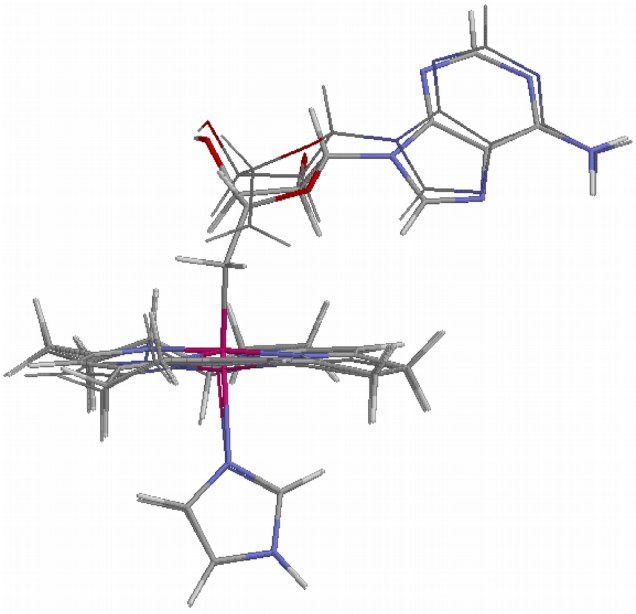

Figure 6. Comparison of the QM/MM optimized Co^{III} (Co–C = 2.0 Å, thick lines) and Co^{II} states (Co–C = 3.5 Å thin lines).

Likewise, we can understand the MM term by dividing it into contributions. The difference in $E_{MM123} - E_{MM1}$ between the

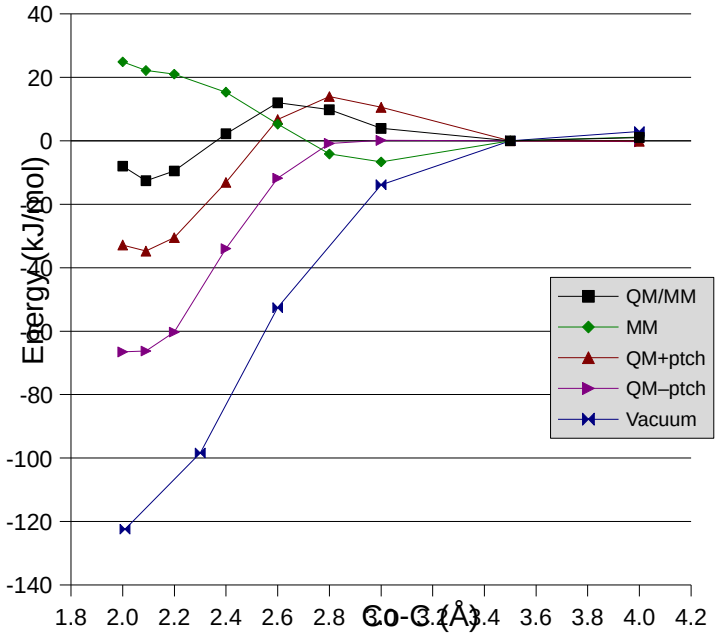

Figure 7. Energy components involved in the Co–C homolytic cleavage in GluMut, using the QM/MM energies with a relaxed protein. The various components are explained in the text. All energies are relative to the one at a Co–C bond length of 3.5 Å.

calculations at Co–C = 2.0 and 3.5 Å is 25 kJ/mol. 5 kJ/mol comes from interactions within system 1, 11 kJ/mol from interactions within system 2 (the interactions within system 3 cancel, because it is fixed), 8 kJ/mol from interactions between systems 1 and 2, whereas the interactions between system 3 and system 1, as well as system 2, are the same in the two states (the first term owing to the large distance between the two systems, but the second term by chance). All the terms are dominated by the electrostatic (not system 1) and van der Waals interactions, although the dihedral terms are often also significant.

Thus, we can conclude that the large protein effect (135 kJ/mol) on the BDE of the Co–C bond can be divided into four contributions: a cage effect (the protein does not allow the Ado radical to dissociate fully from the coenzyme) of 20 kJ/mol, taking us from the BDE (143 kJ/mol) to the vacuum value (122 kJ/mol), a geometric effect from the distortion of the coenzyme of 56 kJ/mol, taking us to the QM–ptch value (66 kJ/mol), an electrostatic effect, arising from improved interactions with the surrounding enzyme in the Co^{II} state, of 34 kJ/mol taking us to the QM+ptch value of 33 kJ/mol, and finally a MM effect from the surrounding enzyme of 25 kJ/mol, taking us finally to the QM/MM value of 8 kJ/mol. These energies are summarized in the first column of Table 3.

However, the interpretation of the results become more intuitive and less technical if we add the 5 kJ/mol from the MM interactions within system 1 (which is mainly a correction for the junctions) to the geometric distortion of this system and the 8 kJ/mol from the MM interaction between systems 1 and 2 to the electrostatic term. Then, we can conclude that the catalysis is caused by cage effects (20 kJ/mol), distortion of the coenzyme (61 kJ/mol), interactions between the coenzyme and the surrounding protein (42 kJ/mol), and improved interactions in the surrounding protein (11 kJ/mol). In the next section, we will try to understand the large geometric term.

Strain in the coenzyme

We have seen that geometric distortions provide most of the catalytic effect in GluMut (56 kJ/mol). The geometric distortion of the quantum system (the coenzyme) can be directly estimated by comparing the energies of the quantum system (without point charges) optimized in the protein and in vacuum, i.e. the "strain energy" ΔE_{QM}. For the Co^{III} state (at Co–C = 2.0 Å), ΔE_{QM} is 229 kJ/mol, indicating that the protein strongly strains AdoCbl. In contrast, ΔE_{QM} for the Co^{II} state is 141 kJ/mol.[88]

Compared to other proteins (ΔE_{QM} = 6–197 kJ/mol),[60,61,78,89,90,91,92,93,94,95] the calculated ΔE_{QM} energy for the Co^{II} state is of a normal magnitude, whereas that of the Co^{III} state of AdoCbl is unusually large. Therefore, we have examined which parts of the AdoCbl cofactor give rise to the large strain. The results in Table 4 shows that excess strain in the Co^{III} state comes almost entirely from the Ado moiety: The strain energy in the Co, imidazole and corrin moieties are rather small and essentially the same in the Co^{II} and Co^{III} states. However, the strain in Ado is 81 kJ/mol higher in Co^{III} than in the Co^{II} state. The majority of this difference (69 kJ/mol) comes from the ribose part of Ado, which is understandable, because it contains two nearby and strong hydrogen bond donors and acceptors (HO2' and HO3'). This is in accordance with the finding that AdoCbl missing the O2' group has only 1–2% of the activity

compared to native coenzyme in MCAM.[96]

We can further understand the strain in the Co^{III} state by truncating Co^{III}CorImAdo to Co^{III}CorImMe by replacing C4' with a hydrogen atom at a distance of 1.10 Å to C5' and deleting the rest of the Ado group. Such a model is 133 kJ/mol less stable than the same model optimized in vacuum. This shows that a significant part of the ribose strain comes from the C5' group alone. If we then optimize only the hydrogen atom that replaced C4', the strain decreases by 38 kJ/mol, showing that Co–C5'–C4' angle was seriously strained (it is 138° in the QM/MM structure, but 119° in both the partly and fully optimized structure). This is probably the most important geometric effect of the protein.

Another way to judge the effect of the various parts of Ado group on the Co–C dissociation, is to repeat the QM/MM optimizations with two other coenzyme models, viz. $CoCorImMe^+$ and $CoCorImRib^+$. The optimized structures of the Co^{III} and Co^{II} states of these systems are described in Table 5. In the Me variant, there are only small geometric changes in the enzyme. In particular, the Co–C–H angle is 110° in the Co^{III} state, like in the optimized vacuum structure. However, the Co–N_{Im} bond is still elongated to 2.59 Å, which shows that the active site is not ideal for binding an *R* group of the coenzyme. In the Rib variant, changes are much larger and similar to those found in AdoCbl.

This is also reflected in the reaction energies shown in Table 3: the Co–C bond is only labilized by 42 kJ/mol in MeCbl (QM/MM – BDE), whereas the labilization with RibCbl (109 kJ/mol) is closer to that of AdoCbl (135 kJ/mol). This difference is caused by a decrease in all four contributions to the labilization, but it is dominated by the geometric and electrostatic terms. In particular, the difference in the ΔE_{QM1} energy between the Co^{III} and Co^{II} states is only 12 kJ/mol for the MeCbl model (88 kJ/mol for AdoCbl). These calculations clearly show why MeCbl cannot be subject to fast homolytic Co–C bond cleavage in mutases:

Table 3. Energy components (kJ/mol) of the Co–C bond cleavage in GluMut with various cofactors.

Contribution[a]	AdoCbl[b]	RibCbl[b]	MeCbl[b]	NoEl[c]	$w_{MM} = 0.01$[d]
BDE	142.5	155.1	159.8	142.5	142.5
Cage	20.1	27.8	9.9	20.1	20.1
Vacuum	122.4	127.3	149.9	122.4	122.4
Geometry	55.9	30.3	11.6	71.4	26.9
QM–ptch	66.5	97.0	138.3	51.0	95.5
Electrostatics	33.7	34.8	12.5	0.0	0.0
QM+ptch	32.9	62.2	125.8	51.0	95.5
MM	24.9	16.1	8.1	19.2	2.8
QM/MM	8.0	46.1	117.7	31.9	92.7
ΔE_{QM1}, 2.0 Å	229.0	161.6	71.2	170.7	38.6
ΔE_{QM1}, 3.5 Å	140.8	97.2	59.2	81.9	4.1

[a] The energy contributions are the QM BDE of the isolated quantum system in vacuum (fully optimized structures), the QM energy of the structures in vacuum (Vacuum), evaluated as the energy difference between the structures optimized at Co–C = 2.0 Å and 3.5 Å (like the following three energies), the QM energy of the QM/MM structures without (QM–ptch) or with (QM+ptch) the point charges, and the total QM/MM energy (QM/MM). MM, Electrostatics, Geometry, and Cage are the difference between the energies on the previous row and the following row. ΔE_{QM1}, 2.0 Å and 3.5 Å are the strain energies for the optimized structures with Co–C fixed to 2.0 and 3.5 Å, respectively.

[b] QM/MM optimizations with AdoCbl, RibCbl, or MeCbl as the cofactors.

[c] QM/MM optimization with AdoCbl as the cofactor and with all point charges zeroed.

[d] QM/MM optimization with AdoCbl as the cofactor, with all point charges zeroed, and w_{MM} set to 0.01 (instead of 1 as in the other calculations).

It simply does not have the polar handle (the Ado group) necessary for the protein to destabilize the Co^{III} state, and the Co–C bond. However, it is also clear that there is a small catalytic effect for MeCbl, which is in accordance with the experimental observation that the Co–C bond cleavage of cobalamins with non-polar *R* groups is accelerated by diol hydratase, although only to a small extent.[97]

What part of the protein distorts AdoCbl?

In the previous sections, we have shown the effect of the enzyme on the Co–C bond cleavage, divided it into contributions, and studied what groups in the coenzyme are important for the catalysis. In this section, we will instead concentrate on the protein and evaluate what interactions and what residues in the protein cause the geometric distortion of the coenzyme. We start by estimating the effect of electrostatic interactions on the distorted geometry. This has been done by simply turning off the electrostatic interactions in the QM/MM optimization.

At Co–C = 2.0 Å, this gave a ΔE_{QM1} of 171 kJ/mol (Table 3, column NoEl), i.e. 58 kJ/mol less than in the corresponding QM/MM structure optimized with the point charges. From this we conclude that electrostatics provide 58 kJ/mol of the total 229 kJ/mol distortion for the Co^{III} state. It can be seen that the catalytic effect (143 – 32 = 111 kJ/mol) has decreased by 24 kJ/mol. The main cause of this effect is of course the absence the electrostatic term, but also the MM term is reduced (there is also electrostatic interactions within system 2 and between systems 2 and 3). Thus, we can conclude that the main effect of electrostatics is direct (polarization of the quantum system) and not indirect, via the geometries.

Consequently, we can conclude that a major part of the geometric distortion of the coenzyme in GluMut, and all the differential destabilization of the Co^{III} state is caused by van der Waals interactions. A way to evaluate this effect is to scale down the MM energies in the QM/MM optimizations by reducing the w_{MM} factor in Eqn. (1). The result of such calculations at w_{MM} = 0.01 is also shown in Table 3. It can be seen that scaling down the van der Waals interactions has a very strong effect on catalysis. At 3.5 Å, the catalytic effect is only 30 kJ/mol (122 – 93). Moreover, the strain energies are very small, 39 kJ/mol for the Co^{III} state and 4 kJ/mol for the Co^{II} state. The low strain energy is accomplished by a reorientation of the HO2' and HO3' atoms and a tilt of the adenine moiety to form three internal hydrogen bonds (Figure S5).

Table 4. Strain in various part of the AdoCbl cofactor.[a]

Strain in	ΔE_{QM1} (kJ/mol)		
	Co^{III}	Co^{II}	Difference $Co^{III} – Co^{II}$
AdoCbl	229.0	140.8	88.2
Ado + Co	121.6	–	
Ado	115.9	34.6	81.3
Rib	97.2	28.6	68.6
Adenine	25.7	3.1	22.6
Corrin + Co	51.6	49.5	2.1
Corrin	48.8	49.1	-0.3
Im + Co	17.8	14.1	3.7
Im	13.3	13.3	0.0

[a] The results were obtained by reoptimizing the quantum system (CoCorImAdo from the QM/MM optimization of GluMut with the Co–C bond fixed to 2.0 and 3.5 Å) in vacuum, keeping various parts of the structure fixed at the QM/MM geometry. The calculations at Co–C = 3.5 Å were done for the Co^{II}CorIm and Ado$^{\bullet}$ parts separately. A residual strain energy of 32.1 and 40.4 kJ/mol has been subtracted from all the Co^{III} energies (except AdoCbl) and from Ado, Rib, and adenine for Co^{II}, respectively (they are caught in a less favorable local minimum).

We can use this calculation to decide which amino acids in the protein cause the geometric distortion by turning on the van der Waals interactions again and finding the major energy terms. The dominating terms come from Thr-94, Asn-123, Lys-326, Glu-330, and a side-chain of coenzyme B_{12} (involving the O28). These residues are shown in Figure 8. Based on these results, we designed a series of in silico mutations of GluMut, in which we removed the side chains of these residues, as well as a few additional residues that are close to the Ado moiety in the crystal structure, viz. Arg-66, Ile-334, and Ala-67 (Asn-123 was not included, because it interacts with its back bone with the coenzyme). The corrin side chain, starting with C26, was replaced by a hydrogen atom.

The ΔE_{QM1} energies relative to the native (not mutated) structure are listed in Table 6. They show only small changes for the individual mutations. The largest reduction of the strain energy (at Co–C = 2.0 Å) is obtained for Glu-330 (–26 kJ/mol), the corrin side chain (–20 kJ/mol), and Lys-326 (–8 kJ/mol). These three

Table 5. Optimized structures of AdoCbl, RibCbl, and MeCbl in vacuum and in GluMut.[a]

Model	Method	Co–C[b]	Co–N_{Im}	Co–N_{Cor}				Fold angle	Co–C–C
AdoCbl	Vacuum	2.01	2.20	1.88	1.88	1.94	1.94	5.1	119.2
	QM/MM	2.00	2.54	1.87	1.92	1.94	1.94	4.9	138.2
		3.50	2.19	1.87	1.90	1.93	1.97	3.0	131.2
RibCbl	Vacuum	2.01	2.21	1.87	1.88	1.94	1.95	4.5	121.6
	QM/MM	2.00	2.60	1.87	1.90	1.92	1.94	5.6	131.4
		3.50	2.26	1.86	1.89	1.92	1.97	4.8	133.9
MeCbl	Vacuum	1.98	2.18	1.88	1.88	1.94	1.94	5.6	110.1
	QM/MM	2.00	2.59	1.86	1.89	1.92	1.95	6.7	109.5
		3.50	2.22	1.86	1.88	1.92	1.96	5.8	99.4

[a] Bond lengths in Å, angles in degrees.
[b] In the vacuum optimizations, the Co–C bond length was fully optimized; in the QM/MM optimizations, the Co–C bond length was fixed to either 2.0 or 3.5 Å.

mutants together (mutant 8) release 46 kJ/mol of strain, suggesting little cooperative effects for these groups. However, all the mutants together (mutant 9) release 83 kJ/mol of strain, which is quite significant and reveals some cooperativity. This is not unexpected, because several mutations may be needed before the Ado moiety can move significantly. The structure of the QM system in the native structure and mutant 10 are compared in Figure 9. It can be seen that the differences are restricted to the Ado group.

However, ΔE_{QM1} for mutant 9 is still quite large. Therefore, we ran another optimization of this mutant with w_{MM} = 0.01 (giving a strain energy of 20 kJ/mol) and looked at the remaining large energy terms. These showed that the substrate and two water molecules still may strain the coenzyme (but no longer Asn-123; cf. Figure 8). The substrate glutamate is especially interesting, because it has been suggested that the cleavage of the Co–C bond is triggered by the binding of the substrate.[40,45] When these three molecules were removed from mutant 9 (giving mutant 10) the strain energy decreased by an additional 42 kJ/mol.

To test that the effect of the mutants is not just a general effect on both sides of the Co–C dissociation equilibrium, we also optimized all mutants for the Co^{II} state. The resulting $\Delta\Delta E_{QM1}$ energies in Table 6 show that the mutants have slightly smaller effects for that state. Lys-326, Glu-330, and the C26 side chain of B_{12} still give the largest net effect on the Co–C bond cleavage. The differential effects of mutants 9 and 10 are 50 and 99 kJ/mol, respectively, showing that these ten groups provide a major part of the enzyme's catalytic effect.[98]

The second reaction step of GluMut: Hydrogen abstraction from glutamate

Finally, we shall briefly discuss also the next steps of the GluMut reaction. The Ado radical has never been observed experimentally and is therefore believed to be very short-lived.[15,24] In fact, isotope effects indicate that at least the first two steps in the GluMut reaction, Co–C bond cleavage and hydrogen atom transfer from the Glu substrate to the Ado$^{\bullet}$ radical, are kinetically coupled.[21,24] Therefore, we have also studied this radical transfer between Glu and Ado, using QM/MM methods, to see if this reaction may significantly change the energetics. This was done by simply optimizing the Ado$^{\bullet}$ + Glu reactant and Ado + Glu$^{\bullet}$ product states, but still including also the full Co^{II}CorIm model in the calculations (in total 102 atoms in the quantum system).

The optimized structures are shown in Figure 10. It can be seen that the cofactor, in particular the corrin ring, is almost unaffected by the reaction. Thus, our results shows that the corrin ring is unimportant from this step. We obtain a reaction energy of 16 kJ/mol, indicating that the Glu$^{\bullet}$ radical is slightly more stable than the Ado$^{\bullet}$ radical. This is similar to what is found for the same reaction in vacuum (without coenzyme B_{12}), 20 kJ/mol. However, if we divide the QM/MM energy into its components, as was done for the Co–C bond cleavage

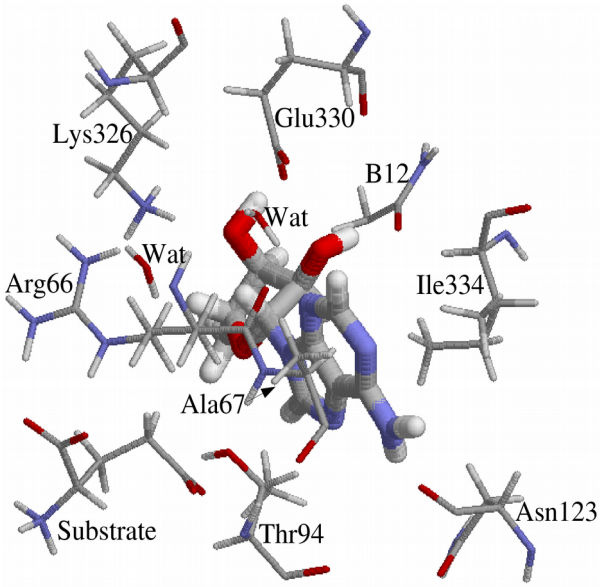

Figure 8. Residues involved in the computational mutations. The Ado group is seen from above coenzyme B_{12}.

above, we see that the reaction is actually disfavored by both the MM (1 kJ/mol) and electrostatics (15 kJ/mol) terms, so that the ΔE_{QC1} result is appreciably more positive (32 kJ/mol) indicating that the Glu• radical is geometrically stabilized in the enzyme over the Ado• radical.

Yet, the main conclusion of this section is that the coupling of the two reactions do not significantly change the reaction energy of the Co–C bond cleavage, so that the results in the previous sections still can be trusted. In particular, the total (QM/MM) reaction energy of the coupled reaction (Co–C bond cleavage and radical transfer) is –8 kJ/mol, i.e. still giving an equilibrium constant close to unity, as is experimentally observed.[14,16,20,21,22] Finally, it might be mentioned that the following rearrangement of Glu• to MeAsp• has been studied before in vacuum,[50] favoring a fragmentation–recombination mechanism, but this step is outside the scope of the present investigation.

Concluding remarks

We have studied the Co–C5' bond dissociation reaction in the enzyme GluMut with QM/MM methods. We have shown that the enzyme strongly affects this reaction. Thus, the BDE of this bond is reduced from 143 kJ/mol in vacuum to 8 kJ/mol in the enzyme in our calculations. This energy is only changed slightly (by 16 kJ/mol) if the Co–C bond cleavage is coupled with the transfer of the radical from Ado to Glu. Moreover, the activation barrier is reduced from 130 kJ/mol to 25 kJ/mol, as can be seen in Figure 5 and Table 2. Thus, our results indicate that the Co–C bond cleavage is not rate-limiting in GluMut, provided that entropy effects are not dominant (our calculations provide only enthalpies, not entropies or free energies). This is in accordance with kinetic measurements on GluMut.[15,20,24] Instead, later steps in the reaction are limiting.

Table 6. AdoCbl strain energies ($\Delta\Delta E_{QM1}$) and reduction of the BDE relative to the native structure in QM/MM optimized mutants.

Mutant	Mutations	$\Delta\Delta E_{QM1}$ (kJ/mol)		Co–C bond
		Co^{III}	Co^{II}	(kJ/mol)
Native	–	0	0	0
1	Lys-326	-8	22	29
2	Glu-330	-26	-15	11
3	Arg-66	1	2	1
4	Thr-94	-3	2	5
5	Ile-334	3	1	-1
6	Ala-67	-1	0	1
7	B_{12}-C26	-20	-1	19
8	330+326+B_{12}-C26	-46	-19	27
9	All the above	-83	-33	50
10	#9+water+substrate	-125	-26	99

We have analyzed in detail how this catalytic effect arises. It can be divided into four components, which all seem to be significant. First, the enzyme keeps the Ado radical bound at a Co–C distance of 3.2–4.2 Å. At this distance the Ado group can still interact favorably with the corrin ring, which reduces the BDE by ~20 kJ/mol (Figure 5 and Table 3). This can be seen as a cage effect.[12]

Second, the enzyme distorts the coenzyme, especially in the Co^{III} state. This differential geometric effect amounts to 61 kJ/mol (including the MM contribution within system 1) and

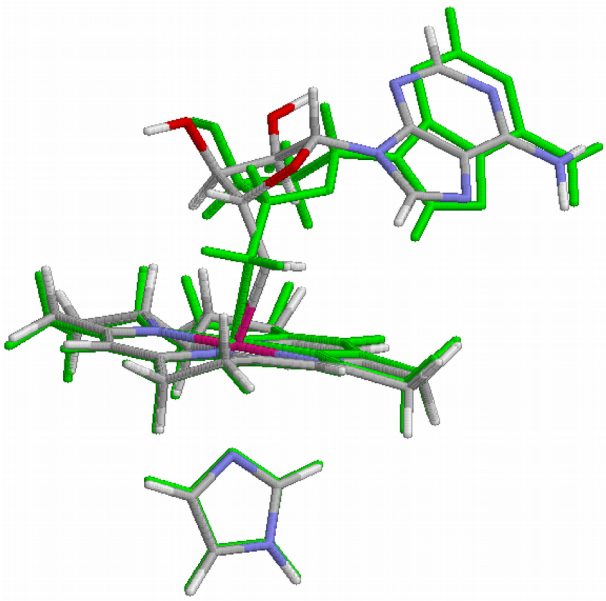

Figure 9. Overlay of QM/MM optimized structures of the Co^{III} state in native GluMut (green) and mutant 10.

is the dominant catalytic component. The differential effect comes mainly from the Rib moiety. The most evident geometric distortion is the Co–C5'–C4' angle, which is changed from 119° in the isolated coenzyme to 138° in the protein. We also obtain a conspicuous elongation of the Co–N_{Im} bond in the Co^{III} state, which is in accordance with many structures of coenzyme B_{12} proteins. However, the 0.3 Å elongation of this bond, destabilizes the complex by less than 4 kJ/mol. This is in accordance with earlier investigations of the effect of the Co–N_{Im} bond on the Co–C BDE.[28,29,55] Thus, the Co–N_{Im} bond cannot explain the catalysis of the enzyme. Instead, the elongation of this bond is a consequence of the enzyme keeping the Ado moiety away from the Co ion by steric interactions.

The third component is the differential stabilization of the Co^{II} state by the surrounding protein. It amounts to 42 kJ/mol and is dominated by electrostatic interactions (i.e. the polarization of the coenzyme by the surrounding protein) with Arg-66, Lys-326, and Asp-14, i.e. to the polar groups surrounding the Ado group.

The fourth component is the stabilization of the surrounding enzyme in the Co^{II} state. It amounts to 11 kJ/mol and comes mainly from van der Waals and electrostatics interactions within the protein.

Furthermore, we have shown that the catalytic effect is not predominantly caused by electrostatic interactions (41 kJ/mol), but rather by van der Waals interaction with the surrounding amino acids. Thus, a mutant in which six amino-acid side chains around the Ado group as well as the substrate, two water molecules and one of the side chains of coenzyme B_{12} have been deleted has a substantially higher BDE than the native enzyme.

Thus, a view emerges from these calculations that the Co–C dissociation reaction is enhanced by the enzyme binding the Co^{II} form of the coenzyme much more favorably than the Co^{III} state. According to crystallographic evidence for both GluMut and MCAM,[40,45,66,65,82] this differential stabilization is caused by a conformational change triggered by the binding the substrate, which essentially destroys the binding site of the Ado moiety and forces it off the coenzyme. This distortion energy is most likely taken from the binding energy of the coenzyme.

There have been much discussion about the two modes of Co–C bond cleavage in B_{12}-dependent enzymes.[45] Our results suggest a reason why MeCbl cannot be used for a radical-generating homolytic reaction: The methyl group has no polar groups and therefore lacks a handle for exerting any of the distorting forces we have observed. This is supported by our results for the MeCbl cofactor in GluMut, which show that the BDE is lowered by only 42 kJ/mol. Instead, the MeCbl coenzyme is used in methyl-transfer reactions, employing the stability of the Co(I) state in a heterolytic reaction and appropriate methyl donors and acceptors.[56,99] We have shown that the methyl-transfer reaction in methionine synthase is enhanced by deprotonation of the homocysteine acceptor and by keeping the active site non-polar,[57] providing a rationale for the hydrophobic nature of the active site of this enzyme.[4] AdoCbl, on the other hand, is too bulky to allow any nucleophilic attack and thereby heterolytic cleavage of the Co–C bond.

Our proposed mechanism for GluMut works most likely also for other AdoCbl enzymes. For example, a similar conformational change has been observed for MCAM[40] and this enzyme has also a Glu residue (Glu-370) that corresponds to Glu-330 in GluMut and forms two hydrogen bonds to ribose O2' and O3'. Likewise, the two hydrogen bonds to adenosine N6 are retained in MCAM[5] (the carbonyl atoms of Glu-91 and Ala-139).

The present study illustrates how theoretical investigations can be used to obtain

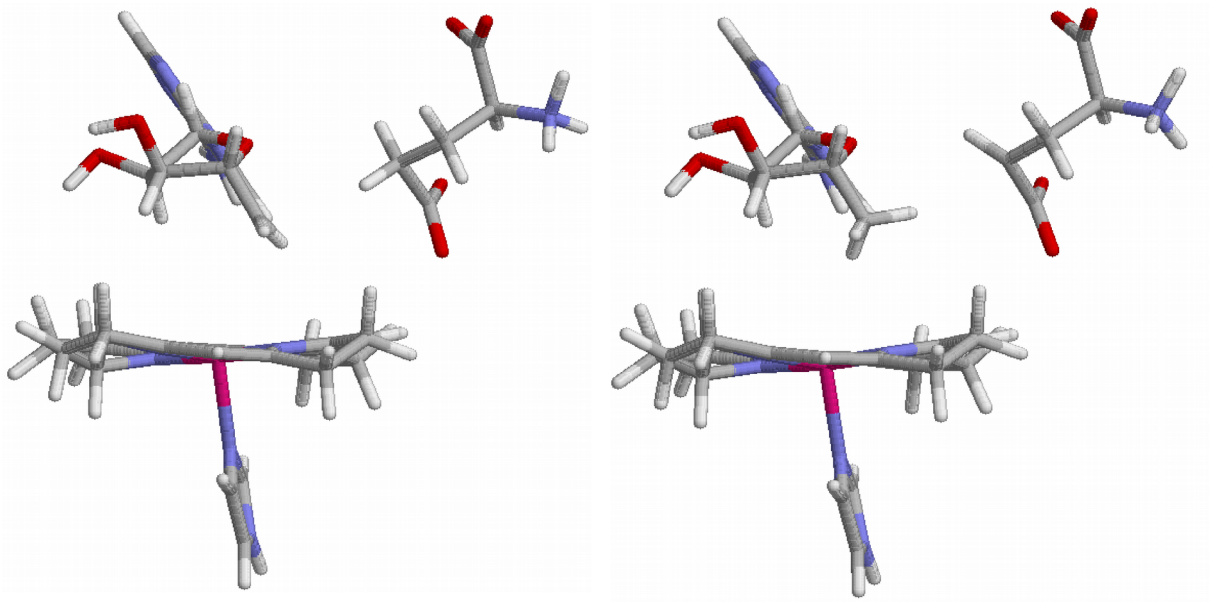

Figure 10. The two states of the radical transfer from Ado to glutamate, optimized in the protein with QM/MM.

detailed information about the catalytic mechanism of enzymes and how various catalytic components may be identified and quantified. We have shown that the catalytic effect comes from the differential stabilization of the Co^{II} state of the coenzyme, but that several energetic components are involved in this stabilization. The results also allow us to completely rule out the mechanochemical trigger mechanism, because nothing happens to the corrin ring during the cleavage of the Co–C bond in the protein.

Acknowledgment

This investigation has been supported by the Swedish research council and by computer resources of Lunarc at Lund University.

Legends to the Figures

Figure 1. The cobalamin system.

Figure 2. Conversion of glutamate to MeAsp, catalyzed by glutamate mutase.

Figure 3. Hydrogen bonds around the Ado moiety in QM/MM optimized structures of conformations B (a; min2) and A (b; min3). The hydrogen bonds are marked out by thin lines.

Figure 4. The QM/MM optimized structure of the Co^{III} state of GluMut B (min1): a) the quantum system; b) hydrogen bond interactions with the Ado group.

Figure 5. Co–C homolytic cleavage in glutamate mutase (QM/MM energy) compared with vacuum energies for $CoCorImAdo^{+}$. The reference energy is at 3.5 Å for the QM/MM curve, but at infinite separation in vacuum.

Figure 6. Comparison of the QM/MM optimized Co^{III} (Co–C = 2.0 Å, thick lines) and Co^{II} states (Co–C = 3.5 Å thin lines).

Figure 7. Energy components involved in the Co–C homolytic cleavage in GluMut, using the QM/MM energies with a relaxed protein. The various components are explained in the text. All energies are relative to the one at a Co–C bond length of 3.5 Å.

Figure 8. The location of residues involved in the computational mutations. The Ado group is seen from above coenzyme B_{12}.

Figure 9. Overlay of QM/MM optimized structures of the Co^{III} state in native GluMut (green) and mutant 10.

Figure 10. The two states of the radical transfer from Ado to glutamate, optimized with QM/MM.

1. Abeles, R. H., and Dolphin, D. (1976) *Acc. Chem. Res.* **9**, 114-120
2. Glusker, J. P. (1995) *Vitamins and Hormons* **50**, 1-76
3. Shibata, N., Masuda, J., Tobimatsu, T., Toraya, T., Suto, K., Morimoto, Y., and Yasuoka, N. (1999) *Structure* **7**, 997-1008
4. Drennan, C. L., Huang, S., Drummond, J. T., Matthews, R. G., and Ludwig, M. L. (1994) *Science* **266**, 1669-1674
5. Mancia, F., Keep, N. H., Nakagawa, A., Leadlay, P. F., McSweeney, S., Rasmussen, B., Bösecke, P., Diat, O. , and Evans, P. R. (1996) *Structure* **4**, 339-350
6. Ludwig, M. L., and Matthews, R. G. (1997) *Annu. Rev. Biochem.* **66**, 269-313
7. Marsh, E. N. G. (2000) *Bioorg. Chem.* **28**, 176-189
8. Golding, B. T., Anderson, R. J., Ashwell, S., Edwards, C. H., Garnett, I., Kroll, F., and Buckel, W. (1998) in: Kräutler, B., Arigoni, D., and Golding, B. T., eds.) *Vitamin B_{12} and the B_{12} proteins*, Wiley-VCH, Weinheim. Chapter 12.
9. Babior, B. M., Carty, T. J., and Abeles, R. H. (1974) *J. Biol. Chem.* **249**, 1689-1695
10. Toraya, T. (2000) *Cell. Mol. Life Sci.* **57**, 106-127
11. Marsh, E. N. G., and Drennan, C. L. (2001) *Curr. Opin. Chem. Biol.* **5**, 499-505
12. Finke, R. G. (1998) in: Kräutler, B., Arigoni, D., and Golding, B. T., eds.) *Vitamin B_{12} and the B_{12} proteins*, Wiley-VCH, Weinheim. Chapter 25.
13. Hay, B. P., and Finke, R. G. (1986) *J. Am. Chem. Soc.* **108**, 4820-4829
14. Brown, K. L., and Zou, X. (1999) *J. Inorg. Biochem.* **77**, 185-195
15. Kratky, C. and Gruber, K. (2001) Handbok of Metalloproteins, 983-994.
16. Padmakumar, R., Padmakumar, R., and Banerjee, R. (1997) *Biochemistry* **36**, 3713-3718
17. Brown, K. L., and Li, J. (1998) J. Am. Chem. Soc. 120, 9466-9474.
18. Licht, S. S., Lawrence, C. C., and Stubbe, J. (1999) *Biochemistry* **38**, 1234-1242
19. Chowdhury, S., and Banerjee, R. (2000) *Biochemistry* **39**, 7998-8006.
20. Marsh, E. N. G., Ballou, D. P. (1998) Biochemistry 37, 11864-11872.
21. Licht, S. S., Booker, S. and Stubbe, J. (1999) *Biochemistry* **38**, 1221-1233.
22. Bandarian, V, Reed, G. H. (2000) Biochemistry 39, 12069-12075.
23. Meier, T. W., Thomä, N. H., Leadlay, P. F. (1996) Biochemistry 35, 11791-11796.
24. Chih, H.-W., Marsh, E. N. G. (1999) Biochemistry 38, 13684-13691.
25. Hill, H. A. O., Pratt, J. M., and R. P. J. Williams (1969) *Chem. Britain.* **5**, 169-172
26. Grate, J. H., and Schrauzer, G. N. (1979) *J. Am. Chem. Soc.* **101**, 4601-4611
27. Halpern, J. (1985) *Science* **227**, 869-875
28. Jensen, K. P., and Ryde, U. (2002) *J. Mol. Struct. (Theochem)* **585**, 239-255
29. Dölker, N., Maseras, F., and Lledos, A. (2001) *J. Phys. Chem. B* **105**, 7564-7571
30. Sirovatka, J. M., Rappé, A. K., and Finke, R. G. (2000) *Inorg. Chim. Acta* **300-302**, 545-555
31. Dong, S. L., Padmakumar, R., Banerjee, R., and Spiro, T. G. (1999) *J. Am. Chem. Soc.* **121**, 7063-7070
32. Scheuring, E., Padmakumar, R., Banerjee, R., and Chance, M. R. (1997) *J. Am. Chem. Soc.* **119**, 12192-12200
33. Tollinger, M., Konrat, R., Hilbert, B. H., Marsh, E. N. G., and Kräutler, B. (1998) *Structure* **6**, 1021-1033
34. De Ridder, D. J. A., Zangrando, E., and Burgi, H.-B. (1996) *J. Mol. Struct.* **374**, 63-83
35. Trommel, J. S., Warncke, K., and Marzilli, L. G. (2001) *J. Am. Chem. Soc.* **123**, 3358-3366
36. Brooks, A. J., Vlasie, M., Banerjee, R., Brunold, T. C. (2004) J. Am. Chem. Soc. 126, 8167-8180.
37. Champloy, F., Jogl, G., Reitzer, R., Buckel, W., Bothe, H., Beatrix, B., Broeker, G., Michalowicz, A., Meyer-Klaucke, W., and Kratky, C. (1999) *J. Am. Chem. Soc.* **121**, 11780-11789
38. Marsh, E. N. G., Holloway, D. E., and Chen, H. P. in: Kräutler, B., Arigoni, D., and Golding, B. T., eds.) *Vitamin B_{12} and the B_{12} proteins*, Wiley-VCH, Weinheim. Chapter 16.
39. Bresciana-Pahor, N., Forcolin, M. Marzilli, L. G., Randaccio, L., Summers, M. F., Toscano, P. J. (1985) Coord. Chem. Rev. 63, 1-47.
40. Mancia, F., Evans, P. R. (1998) Structure, 6, 711-720.
41. Vlasie, M. D.., Banerjee, R. (2003) J. Am. Chem. Soc. 125, 5431-5435.
42. N.H. Thomä, T.W. Meier, P.R. Evans, P.F. Leadlay, Biochemistry 37 (1998) 14386
43. Toraya, T., Ishida, A. (1988) Biochemistry 27, 7677-7682.
44. Zhu, L., Kostic, N. M. (1987) 26, 6-15.
45. R. Banerjee, Chemistry & Biology, 4 (1997) 175-186.
46. DM Smith, BT Golding, L Radom, J. Am. Chem. Soc. 1999, 121, 1037-1044
47. DM Smith, BT Golding, L Radom, J. Am. Chem. Soc. 1999, 121, 1383-1384
48. DM Smith, BT Golding, L Radom, J. Am. Chem. Soc. 1999, 121, 9388-9399
49. S. D. Wetmore, DM Smith, L Radom, ChemBioChem 2001, 2, 919-922
50. S. D. Wetmore, DM Smith, BT Golding, L Radom, J. Am. Chem. Soc. 2001, 123, 7963-7972

51. M. J. Loferer, B. M. Webb, G. H. Brand, K. R. Liedl (2003) J. Am. Chem. Soc. 125, 1072-1078.
52. T. Kamaschi, T. Toraya, K. Yoshizawa (2004) J. Am. Chem. Soc., ASAP article.
53. K. P. Jensen, S. P. A. Sauer, T. Liljefors, P.-O. Norrby, Organometallics 2001, 20(3), 550-556
54. T. Andruniow, M. Z. Zgierski, and P. M. Kozlowski, Chem. Phys. Lett., 331 (2000) 509
55. T. Andruniow, M. Z. Zgierski, and P. M. Kozlowski, J. Am. Chem. Soc., 123 (2001) 2679.
56. K. P. Jensen, U. Ryde, ChemBioChem 2003, 4, 413-424
57. K. P. Jensen, U. Ryde, J. Am. Chem. Soc. 2003, 125(46); 13970-13971
58. Freindorf, M.; Kozlowski, P. M. J. Am. Chem. Soc. 2004; 126(7); 1928-1929
59. Gruber, K. and Kratky, C., (2002) Curr. Opin. Chem. Biol. 6, 598-603.
60. U. Ryde, J. Comput.-Aided Mol Design 10 , 1996, 153-164
61. U. Ryde & M. H. M. Olsson (2001) Intern. J. Quant. Chem., 81, 335-347.
62. Reuter N, Dejaegere A, Maigret B, Karplus M. J Phys Chem A 2000, 104:1720-1735.
63. Cornell, W. D.; Cieplak, PI.; Bayly, C. I.; Gould, I. R.; Merz, K. M.; Ferguson, D. M.; Spellmeyer, D. C.; Fox, T.; Caldwell, J. W.; Kolman, PI.. A. *J. Am. Chem. Soc.* **1995**, *117*, 5179-5197.
64. Svensson, M., Humbel, S., Froese, R. D. J., Matsubara, T., Sieber, S., Morokuma, K. J Phys Chem 1996, 100, 19357.
65. K Gruber, R Reitzer, C Kratky, Angew. Chem. Int. Ed. 2001, 40, 3377-3380
66. R. Reitzer, K. Gruber, G. Jogl, U. G. Wagner, H. Bothe, W. Buckel, and C. Kratky, Structure, 7 (1999) 891
67. E N G Marsh, DE Holloway, H-P Chen, in: (B Kräutler, D Arigoni, BT Golding, eds.) *Vitamin B_{12} and the B_{12} proteins*, Wiley-VCH, Weinheim, 1998. Chapter 16
68. Cornell, W. D.; Cieplak, PI.; Bayly, C. I.; Gould, I. R.; Merz, K. M.; Ferguson, D. M.; Spellmeyer, D. C.; Fox, T.; Caldwell, J. W.; Kolman, PI.. A. *J. Am. Chem. Soc.* **1995**, *117*, 5179-5197.
69. H.M.Marques, B Ngoma, TJ Egan, K.L. Brown, J Mol Struct. Theochem 2001, 561, 71-91.
70. R. Alrichs, M. Bär, M. Häser, H. Horn, C. Kölmel, *Chem. Phys. Lett.* **1989**, *162*, 165
71. Turbomole, version 5.6., by Karlsruhe University, Dept. Theoretical Chemistry, 2001
72. A. Schäfer, H. Horn, R. Ahlrichs, *J. Chem. Phys.* **1992**, *97*, 2571
73. Eichkorn, K., Treutler, O., H. Öhm, M. Häser, Ahlrichs, R. Chem. Phys. Lett., 240 (1995) 283-290.
74. Eichkorn, K.; Weigend, F.; Treutler, O.; Ahlrichs, R. Theor. Chem. Acc. 1997, *97*, 119-124.
75. K. P. Jensen, U. Ryde, J. Phys. Chem B. 2003, 107(38), 7539-7545
76. A. D. Becke, *Phys. Rev. A* **1988**, *38*, 3089
77. J. P. Perdew, *Phys. Rev. B* **1986**, *33*, 8822
78. U. Ryde, In: Recent Research Developments in Protein Engineering. Research Signpost: Trivandrum, India, pp. 65-91, 2002.
79. L Ouyang, P Rulis, WY Ching, G Nardin, L Randaccio, Inorg. Chem. 2004, 43, 1235-1241.
80. B Kräutler, W Keller, C Kratky, J. Am. Chem. Soc. 1989, 111, 8936-8938.
81. S. Dong, R. Padmakumar, N. Maita, R. Banerjee, and T. G. Spiro, J. Am. Chem. Soc., 120 (1998) 9947-9948
82. F Mancia, GA Smith, PR Evans, Biochemistry, 1999, 38, 7999-8005
83. N Dölker, F Maseras, PEM Siegbahn, Chem Phys Lett. 2004, 386, 174-178
84. It should be noted that the experimental BDE of MeCbl is 155±13 kJ/mol[85,] in good agreement with our theoretical estimate (160 kJ/mol). However, our estimate of the BDE in CoCorImAdo, 143 kJ/mol, is quite different from that of AdoCbl, 126 ± 8 kJ/mol.[12,13] This difference cannot be attributed to the change of the axial ligand from Im to 5,6-dimethylbenzimidazole, which is actually predicted to increase the BDE, but only by 1 kJ/mol.[28,75] This discrepancy remains to be explained, but it is possible that the Ado radical does not fully dissociate from the corrin ring in the experiment (cage effects), so that what is actually measured for AdoCbl is only the dissociation curve to a finite distance (~4 Å), as is shown in Figure 3, explaining the difference between MeCbl and AdoCbl. This is supported by the fact that the Co–C bond distances in the two coenzymes are almost the same (within 0–0.05 Å), both in calculations and experiments[29,75,79,], although a linear relation has been established between the Co–C bond length and the BDE.[53,55] In the following discussions, we will ignore this discrepancy between experiments and calculations and use our calculated values, to make the discussion more clear.
85. Martin, B. D. ; Finke, R. G. *J. Am. Chem. Soc.* **1990**, *112*, 2419-2420.
86. The QM/MM Co^{III} energy minimum (min1) is shifted to a Co–C bond length of 2.08 Å, compared to 2.01 Å for the isolated cofactor. However, the QM/MM energy is only 5 kJ/mol higher at 2.00 Å than in min1, indicating that this part of the potential surface is flat. Therefore, it is not clear whether the Co–C bond is elongated in the Co^{III} state of the enzyme or not, and if it is elongated, the effect is not large, in accordance with experimental suggestions.[36] This shows that the Co^{III} can be strongly destabilized although it is not reflected in a long Co–C bond.
87. It should be noted that this term does not include the differential stabilization of the Co^{II} state by CoCorImAdo itself (i.e. hydrogen bonds within the QM system, but it includes the stabilization by the Cor side chains, which are not in the quantum system).
88. The Co^{II} state was divided into the Co(II)Cbl + Ado$^{\bullet}$ parts, using the corresponding isolated molecules as the reference states. ΔE_{QM1} of the two parts was 66 and 75 kJ/mol. If we instead use Co^{III}CorAdo as the reference

state, the strain energy is 296 kJ/mol, the difference being the BDE.
89. U. Ryde (1995) Prot. Sci. 4, 1124-1132.
90. U. Ryde (1996) Eur. J. Biophys. 24, 213-221.
91. E. Sigfridsson, M. H. M. Olsson, U. Ryde (2001) Inorg. Chem. 40, 2509-2519.
92. E. Sigfridsson, U. Ryde (2002) J. Inorg. Biochem. 91, 101-115.
93. E. Sigfridsson, U. Ryde (2003) J. Biol. Inorg. Chem. 8, 273-282.
94. U. Ryde & K. Nilsson (2003) J. Mol. Struct. (Theochem), 632, 259-275.
95. Torrent M., Vreven T., Musaev D. G., Morokuma K. (2001) J. Am. Chem. Soc. 124, 192-193.
96. A. M. Calafat, S. Taoka, J. M. Puckett C. Semerad, H. Yan, L. Luo, H. Chen, R. Banerjee, L. G. Marzilli (1995), Biochemistry 34, 14125-14130.
97. T. Toraya, A. Ishida (1988) Biochemistry, 27, 7677-7681.
98. In fact, 99 kJ/mol is larger than the geometry contribution in Table 3, 57 kJ/mol, because the mutants were only run with system 2 fixed, to make the calculations faster and more stable.
99. K. P. Jensen, U. Ryde, submitted to J. Phys. Chem. B.

TOC graphics.

The energy of the Co–C bond cleavage in glutamate mutase divided into components based on QM/MM calculations.